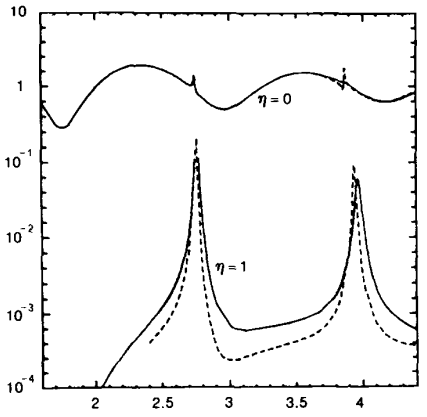

Fig. 4. Normalized backscattering cross section $\sigma/(\pi a^2)$ in range $ka = 1.6$–4.4, for metal sphere ($\eta = 0$) and for perfectly absorbing sphere ($\eta = 1$). Solid line: $M = 21$; dashed line: $M = 41$.

eliminates some of the spurious internal resonances of the scatterer [28].

IV. Conclusion

We have developed and tested a computer code for calculating the surface electric current density induced by a plane wave axially incident on a body of revolution with an impedance boundary condition. Apart from internal resonances, the computations yield accurate results well into the high-frequency region, where asymptotic techniques become applicable. If the surface impedance varies along the profile of the scatterer, the code can still be used by using a (piecewise) linear approximation for the relative surface impedance η on the $(M - 1)$ intervals of the profile. A formula has been obtained for the bistatic far field.

Acknowledgment

The authors wish to thank Prof. V. Daniele of the Politecnico di Torino for helpful discussions.

References

[1] M. G. Andreasen, "Scattering from bodies of revolution," *IEEE Trans. Antennas Propagat.*, vol. AP-13, pp. 303–310, 1965.

[2] J. R. Mautz and R. F. Harrington, "Radiation and scattering from bodies of revolution," *Appl. Sci. Res.*, vol. 20, pp. 405–435, 1969.

[3] P. L. E. Uslenghi, "Computation of surface currents on bodies of revolution," *Alta Frequenza*, vol. 39, pp. 709–720, 1970.

[4] J. R. Mautz and R. F. Harrington, "An improved *E*-field solution for a conducting body of revolution," Syracuse Univ., Syracuse, NY, Rep. TR-80-1, Jan. 1980.

[5] ——, "An *H*-field solution for a conducting body of revolution," Syracuse Univ., Syracuse, NY, Rep. TR-80-6, Sept. 1980.

[6] ——, "*H*-field, *E*-field and combined field solutions for bodies of revolution," Syracuse Univ., Syracuse, NY, Rep. TR-77-2, Feb. 1977.

[7] W. V. T. Rusch and R. J. Pogorzelski, "A mixed field solution for scattering from composite bodies," *IEEE Trans. Antennas Propagat.*, vol. AP-34, pp. 955–958, 1986.

[8] T. K. Sarkar and S. M. Rao, "A simple technique for solving *E*-field integral equations for conducting bodies at internal resonances," *IEEE Trans. Antennas Propagat.*, vol. AP-30, pp. 1250–1254, 1982.

[9] A. W. Glisson and D. R. Wilton, "Simple and efficient numerical techniques for treating bodies of revolution," Rome Air Development Center, Griffiss AFB, NY, Rep. RADC-TR-79-22, Mar. 1979.

[10] L. N. Medgyesi-Mitschang and D. S. Wang, "Hybrid solutions for scattering from perfectly conducting bodies of revolution," *IEEE Trans. Antennas Propagat.*, vol. AP-31, pp. 570–583, 1983.

[11] J. R. Mautz and R. F. Harrington, "Electromagnetic scattering from a homogeneous body of revolution," Syracuse Univ., Syracuse, NY, Rep. TR-77-10, Nov. 1977.

[12] ——, "Electromagnetic scattering from a homogeneous material body of revolution," *Arch. Elek. Übertragung.*, vol. 33, pp. 71–80, 1979.

[13] L. N. Medgyesi-Mitschang and C. Eftimiu, "Scattering from axisymmetric obstacles embedded in axisymmetric dielectrics: the method of moment solution," *Appl. Phys.*, vol. 19, pp. 275–285, 1979.

[14] R. J. Garbacz, "Bistatic scattering from a class of lossy dielectric spheres with surface impedance boundary conditions," *Phys. Rev.*, vol. 133, pp. A14–A16, 1964.

[15] J. R. Wait and C. M. Jackson, "Calculations of the bistatic scattering cross section of a sphere with an impedance boundary condition," *Radio Sci. J. Res. Nat. Bur. Stand./USNC-URSI*, vol. 69D, pp. 299–314, Feb. 1965.

[16] V. H. Weston and R. Hemenger, "High frequency scattering from a coated sphere," *J. Res. Nat. Bur. Stand.*, vol. 66D, pp. 613–619, 1962.

[17] N. G. Alexopoulos and P. L. E. Uslenghi, "Antennas on spheroids with a variable surface impedance," URSI Fall Meeting, Columbus, OH, Sept. 1970.

[18] N. G. Alexopoulos, G. A. Tadler, and P. L. E. Uslenghi, "Scattering from spheroidal composite objects," *J. Franklin Inst.*, vol. 309, pp. 147–162, 1980.

[19] K. M. Mitzner, "An integral equation approach to scattering from a body of finite conductivity," *Radio Sci.*, vol. 2, pp. 1459–1470, 1967.

[20] K. A. Iskander, L. Shafai, A. Frandsen, and J. E. Hansen, "Application of impedance boundary conditions to numerical solution of corrugated circular horns," *IEEE Trans. Antennas Propagat.*, vol. AP-30, pp. 366–372, 1982.

[21] L. N. Medgyesi-Mitschang and J. M. Putnam, "Integral equation formulations for imperfectly conducting scatterers," *IEEE Trans. Antennas Propagat.*, vol. AP-33, pp. 206–214, Feb. 1985.

[22] J. R. Rogers, "On combined source solutions for bodies with impedance boundary conditions," *IEEE Trans. Antennas Propagat.*, vol. AP-33, pp. 462–465, Apr. 1985.

[23] L. N. Medgyesi-Mitschang and D. S. Wang, "Hybrid solutions for large-impedance coated bodies of revolution," *IEEE Trans. Antennas Propagat.*, vol. AP-34, pp. 1319–1329, Nov. 1986.

[24] J. R. Rogers, "Comments on 'integral equation formulations for imperfectly conducting scatterers' and reply by the authors," *IEEE Trans. Antennas Propagat.*, vol. AP-33, pp. 1283–1284, Nov. 1985.

[25] J. A. Ducmanis and V. V. Liepa, "Surface field components for a perfectly conducting sphere," Radiation Lab., Univ. of Michigan, Ann Arbor, Rep. 5548-3-T, Mar. 1965.

[26] V. H. Weston, "Theory of absorbers in scattering," *IEEE Trans. Antennas Propagat.*, vol. AP-11, pp. 578–584, 1963.

[27] R. D. Graglia and P. L. E. Uslenghi, "Electromagnetic scattering by impedance bodies of revolution," presented at the Nat. Radio Science Meeting, Houston, TX, May 1983.

[28] J. Van Bladel, *Electromagnetic Fields*. New York: McGraw-Hill, 1964.

Differential Cross Section of a Dielectric Ellipsoid by the *T*-Matrix Extended Boundary Condition Method

JOHN B. SCHNEIDER AND IRENE C. PEDEN, FELLOW, IEEE

***Abstract*—The extended boundary condition method (EBCM) is applied to the ellipsoidal dielectric scatterer, thus making possible the analytical treatment of a broader class of targets than has been previously**

Manuscript received June 16, 1987; revised January 20, 1988. This work was supported by National Science Foundation Grant NSF 8408046.

The authors are with the Department of Electrical Engineering, FT-10, University of Washington, Seattle, WA 98195.

IEEE Log Number 8821483.

available under a rotational symmetry constraint. Expressions are presented and calculated results provided for an ellipsoid in the resonant range; comparison is made with an oblate spheroid that is comparable in terms of volume.

I. Introduction

There is considerable current interest in the detection and identification of dielectric targets over a wide range of physical dimensions. Applications include scattering from raindrops, hailstones, or other ice objects of varying sizes and degrees of irregularity, optical fibers, imperfections in dielectric substrates, buried cavities, tunnels, plastic pipes, and other objects having geophysical, military, biological, or other practical significance. The ellipsoidal formulation shows promise for categorizing some irregular dielectric target shapes and may be particularly useful when such targets are buried in lossy materials, given that higher frequencies are preferentially attenuated in such media with possible related loss of information about scattering from portions of the boundary having small radii of curvature. The ellipsoidal result is applicable when three-dimensional scattering problems are to be addressed or approximated.

The extended boundary condition method (EBCM) has been used successfully to solve for the electromagnetic fields scattered from a single object when its size is on the order of a wavelength of the illumination. The class of dielectric objects reported has been restricted to those having rotational symmetry about an axis, e.g., prolate and oblate spheroids. Waterman [1], Barber [2], Yeh *et al.* [3], Barber *et al.* [4], and Holt [5], [6] are among those who have reported such results. Mugnai and Wiscombe [7] used EBCM to solve for the scattering cross section of a particle whose radius was given by a Chebyshev polynomial.

The presence of a dielectric body is associated with volume distributions of currents in the medium. The resulting volume integral equations are applicable to arbitrary inhomogeneous dielectrics, but they require solution of six scalar three-dimensional integral equations. The EBCM provides an alternative to the surface integral formulation and its variants by focusing attention on the interior integral equation. Reduction of the computational effort is an important issue in dealing with integral equations. To this end, integral equation methods have been combined with finite difference techniques. Kristensson and Ström [8] and Karlsson and Kristensson [9] are among those who have obtained solutions for a general three-dimensional treatment of electromagnetic scattering for an inhomogeneity inside a stratified half-space by means of the related T matrix method.

This communication describes the result of applying the EBCM to dielectric ellipsoids which, in general, have no rotational symmetry. It represents a step in a more general study of single-object scattering in the resonant range that has the goal of extending the practical applications to a wider class of targets, including irregular shapes that can be described in terms of a "best fit" ellipsoid.

II. General Method

Following Tsang *et al.* [10], the incident and scattered fields are first expanded in a series of basis functions, with vector spherical wave functions, regular at the origin, used to represent the incident field.

$$Rg\bar{M}_{mn}(kr,\theta,\phi)=\gamma_{mn}j_n(kr)\left(\hat{\theta}\frac{jm}{\sin\theta}P_n^m(\cos\theta)-\hat{\phi}\frac{dP_n^m(\cos\theta)}{d\theta}\right)e^{jm\phi} \quad (1)$$

$$Rg\bar{N}_{mn}(kr,\theta,\phi)=\gamma_{mn}\left(\hat{r}\frac{n(n+1)}{kr}j_n(kr)P_n^m(\cos\theta)+\frac{1}{kr}\frac{d(krj_n(kr))}{dkr}\left[\hat{\theta}\frac{dP_n^m(\cos\theta)}{d\theta}+\hat{\phi}\frac{jm}{\sin\theta}P_n^m(\cos\theta)\right]\right)e^{jm\phi} \quad (2)$$

where

$$\gamma_{mn}=\left(\frac{(2n+1)(n-m)!}{4\pi n(n+1)(n+m)!}\right)^{1/2},$$

k is the free-space wavenumber, j_n is the spherical Bessel function, and P_n^m is the associated Legendre polynomial. The mn subscript is uniquely mapped into a single numerical subscript by means of the expression

$$l=n(n+1)+m.$$

Further practical considerations dictate limiting n to $N_{\max}$, which remains to be selected in any given case.

The outgoing vector spherical waves $\bar{M}_{mn}(kr,\theta,\phi)$ and $\bar{N}_{mn}(kr,\theta,\phi)$ are used as the basis functions for the scattered field, with the spherical Hankel function h_n replacing j_n in (1) and (2). The relationship of the unknown scattered field coefficients to those of the incident field, which are known, is expressed as follows:

$$\bar{a}^s=\bar{T}\bar{a}^{\text{inc}}. \quad (3)$$

$\bar{T}$ is the transition or T matrix, and $\bar{a}^{\text{inc}}$ and $\bar{a}^s$ are column vectors of incident and scattered field coefficients, respectively, with dimensions $2L_{\max}\times 1$ where $L_{\max}=N_{\max}(N_{\max}+2)$; the dimensions of $\bar{T}$ are $2L_{\max}\times 2L_{\max}$.

The T matrix depends only on properties of the scattering object and the frequency of illumination. Determination of the T matrix provides a solution to the scattering problem. To obtain it, the incident and scattered fields are individually related to the surface fields of the scattering object and the resulting equations combined to yield the expression

$$\bar{T}=-Rg\bar{Q}^t(\bar{Q}^t)^{-1} \quad (4)$$

where $\bar{Q}^t$ is

$$\bar{Q}^t=\begin{bmatrix}\bar{P} & \bar{R}\\ \bar{S} & \bar{U}\end{bmatrix} \quad (5)$$

and

$$P_{ll'}=P_{mnm'n'}=-jkk_sJ^{(21)}_{mnm'n'}-jk^2J^{(12)}_{mnm'n'} \quad (6)$$

$$R_{ll'}=R_{mnm'n'}=-jkk_sJ^{(11)}_{mnm'n'}-jk^2J^{(22)}_{mnm'n'} \quad (7)$$

$$S_{ll'}=S_{mnm'n'}=-jkk_sJ^{(22)}_{mnm'n'}-jk^2J^{(11)}_{mnm'n'} \quad (8)$$

$$U_{ll'}=U_{mnm'n'}=-jkk_sJ^{(12)}_{mnm'n'}-jk^2J^{(21)}_{mnm'n'} \quad (9)$$

$$J^{(11)}_{mnm'n'}=(-1)^m\int_S dS\hat{n}(\bar{r})\cdot Rg\bar{M}_{m'n'}(k_sr,\theta,\phi)\times\bar{M}_{-mn}(kr,\theta,\phi) \quad (10)$$

$$J^{(12)}_{mnm'n'}=(-1)^m\int_S dS\hat{n}(\bar{r})\cdot Rg\bar{M}_{m'n'}(k_sr,\theta,\phi)\times\bar{N}_{-mn}(kr,\theta,\phi) \quad (11)$$

$$J^{(21)}_{mnm'n'} = (-1)^m \int_S dS\hat{n}(\bar{r}) \cdot Rg\bar{N}_{m'n'}(k_s r, \theta, \phi) \times \bar{M}_{-mn}(kr, \theta, \phi) \quad (12)$$

$$J^{(22)}_{mnm'n'} = (-1)^m \int_S dS\hat{n}(\bar{r}) \cdot Rg\bar{N}_{m'n'}(k_s r, \theta, \phi) \times \bar{N}_{-mn}(kr, \theta, \phi). \quad (13)$$

S is the surface bounding the object, $\hat{n}$ is the outward normal, and k_s is the wavenumber of the scattering object. $Rg\bar{Q}^t$ is the same as $\bar{Q}^t$ but with $\bar{M}_{mn}$ and $\bar{N}_{mn}$ replaced by $Rg\bar{M}_{mn}$ and $Rg\bar{N}_{mn}$, respectively.

For objects whose surface points are given by $r(\theta, \phi)$, an incremental area of the surface is given by

$$dS\hat{n}(\bar{r}) = r^2 \sin\theta \bar{\sigma}(\bar{r}) d\theta d\phi \quad (14)$$

where

$$\bar{\sigma}(\bar{r}) = \hat{r} - \hat{\theta}\frac{1}{r}\frac{\partial r}{\partial \theta} - \hat{\phi}\frac{1}{r\sin\theta}\frac{\partial r}{\partial \theta}. \quad (15)$$

Waterman [1] has shown that the scattering matrix for a lossless particle is unitary. The scattering and T matrices are related by

$$\bar{S} = \bar{I} + 2\bar{T}$$

where $\bar{I}$ is the unit matrix. It follows that a check of the unitarity of the scattering matrix provides a quick check of a computer program written to obtain the T matrix for a lossless particle.

III. Formulation for an Ellipsoid

Making use of the equation for an ellipsoidal surface, $r(\theta, \phi)$ is given by

$$r(\theta, \phi) = \left[\sin^2\theta\left(\frac{\cos^2\phi}{a^2} + \frac{\sin^2\phi}{b^2}\right) + \frac{\cos^2\theta}{c^2}\right]^{1/2} \quad (16)$$

which leads to

$$\bar{\sigma}(\bar{r}) = \hat{r} + \hat{\theta}r^2\left(\frac{\cos^2\phi}{a^2} + \frac{\sin^2\phi}{b^2} - \frac{1}{c^2}\right)\sin\theta\cos\theta + \hat{\phi}r^2\left(-\frac{1}{a^2} + \frac{1}{b^2}\right)\sin\phi\cos\phi\sin\theta. \quad (17)$$

The T matrix is then found by incorporating these two equations in (4)–(14). Symmetry in the integrands of (10)–(13) can be exploited to reduce the computation as explained in the next section.

The terms $J^{(11)}$, $J^{(12)}$, $J^{(21)}$, and $J^{(22)}$ can be written for the ellipsoid as follows:

$$J^{(11)}_{mnm'n'} = -(-1)^m[1+(-1)^{m'-m}][1+(-1)^{n'+n+1}] \cdot \int_0^{\pi} d\phi \int_0^{\pi/2} d\theta r^2 \sin\theta \gamma_{m'n'}\gamma_{-mn} \cdot e^{j\phi(m'-m)} j_{n'}(k_s r) h_n(kr) \left(\frac{jm'}{\sin\theta} P^{m'}_{n'}(\cos\theta) \cdot \frac{dP^{-m}_n(\cos\theta)}{d\theta} + \frac{dP^{m'}_{n'}(\cos\theta)}{d\theta}\frac{jm}{\sin\theta}P^{-m}_n(\cos\theta)\right) \quad (18)$$

$$J^{(12)}_{mnm'n'} = -(-1)^m[1+(-1)^{m'-m}][1+(-1)^{n'+n}] \cdot \int_0^{\pi} d\phi \int_0^{\pi/2} d\theta r^2 \sin\theta \gamma_{m'n'}\gamma_{-mn} \cdot e^{j\phi(m'-m)} j_{n'}(k_s r) \left\{\frac{1}{kr}\frac{d(krh_n(kr))}{dkr} \cdot \left(\frac{jm'}{\sin\theta}P^{m'}_{n'}(\cos\theta)\frac{jm}{\sin\theta}P^{-m}_n(\cos\theta) - \frac{dP^{m'}_{n'}(\cos\theta)}{d\theta}\frac{dP^{-m}_n(\cos\theta)}{d\theta}\right) + n(n+1)\frac{h_n(kr)}{kr}P^{-m}_n(\cos\theta)r^2\sin\theta \cdot \left[\left(\frac{\cos^2\phi}{a^2} + \frac{\sin^2\phi}{b^2} - \frac{1}{c^2}\right)\cos\theta\frac{dP^{m'}_{n'}(\cos\theta)}{d\theta} + \left(-\frac{1}{a^2} + \frac{1}{b^2}\right)\sin\phi\cos\phi\frac{jm'}{\sin\theta}P^{m'}_{n'}(\cos\theta)\right]\right\} \quad (19)$$

$$J^{(21)}_{mnm'n'} = -(-1)^m[1+(-1)^{m'-m}][1+(-1)^{n'+n}] \cdot \int_0^{\pi} d\phi \int_0^{\pi/2} d\theta r^2 \sin\theta \gamma_{m'n'}\gamma_{-mn} \cdot e^{j\phi(m'-m)} h_n(kr) \left\{\frac{1}{k_s r}\frac{d(k_s r j_{n'}(k_s r))}{dk_s r} \cdot \frac{jm'}{\sin\theta}P^{m'}_{n'}(\cos\theta)\frac{jm}{\sin\theta}P^{-m}_n(\cos\theta) - \frac{dP^{m'}_{n'}(\cos\theta)}{d\theta}\frac{dP^{-m}_n(\cos\theta)}{d\theta} + n'(n'+1)\frac{j_{n'}(k_s r)}{k_s r}P^{m'}_{n'}(\cos\theta)r^2\sin\theta \cdot \left[\left(\frac{\cos^2\phi}{a^2} + \frac{\sin^2\phi}{b^2} - \frac{1}{c^2}\right)\cos\theta\frac{dP^{-m}_n(\cos\theta)}{d\theta} - \left(-\frac{1}{a^2} + \frac{1}{b^2}\right)\sin\phi\cos\phi\frac{jm}{\sin\theta}P^{-m}_n(\cos\theta)\right]\right\} \quad (20)$$

$$J^{(22)}_{mnm'n'} = -(-1)^m[1+(-1)^{m'-m}][1+(-1)^{n'+n+1}] \cdot \int_0^{\pi} d\phi \int_0^{\pi/2} d\theta r^2 \sin\theta \gamma_{m'n'}\gamma_{-mn} \cdot e^{j\phi(m'-m)} \left[\frac{1}{k_s r}\frac{d(k_s r j_{n'}(k_s r))}{dk_s r} \cdot \frac{1}{kr}\frac{d(krh_n(kr))}{dkr}\right.$$

$$\cdot \left(\frac{dP_{n'}^{m'}(\cos\theta)}{d\theta} \frac{jm}{\sin\theta} P_n^{-m}(\cos\theta) + \frac{jm'}{\sin\theta} P_{n'}^{m'}(\cos\theta) \frac{dP_n^{-m}(\cos\theta)}{d\theta} \right)$$

$$- r^2 \left(\frac{\cos^2\phi}{a^2} + \frac{\sin^2\phi}{b^2} - \frac{1}{c^2} \right) \sin\theta \cos\theta$$

$$\cdot \left(\frac{1}{k_s r} \frac{d(k_s r j_{n'}(k_s r))}{dk_s r} \frac{jm'}{\sin\theta} \cdot P_{n'}^{m'}(\cos\theta) n(n+1) \frac{h_n(kr)}{kr} P_n^{-m}(\cos\theta) + n'(n'+1) \frac{j_{n'}(k_s r)}{k_s r} P_{n'}^{m'}(\cos\theta) \frac{1}{kr} \cdot \frac{d(krh_n(kr))}{dkr} \frac{jm}{\sin\theta} P_n^{-m}(\cos\theta) \right)$$

$$- r^2 \left(-\frac{1}{a^2} + \frac{1}{b^2} \right) \sin\phi \cos\phi \sin\theta$$

$$\cdot \left(n'(n'+1) \frac{j_{n'}(k_s r)}{k_s r} P_{n'}^{m'}(\cos\theta) \cdot \frac{1}{kr} \frac{d(krh_n(kr))}{dkr} \frac{dP_n^{-m}(\cos\theta)}{d\theta} - n(n+1) \cdot \frac{1}{k_s r} \frac{d(k_s r j_{n'}(k_s r))}{dk_s r} \frac{dP_{n'}^{m'}(\cos\theta)}{d\theta} \cdot \frac{h_n(kr)}{kr} P_n^{-m}(\cos\theta) \right) \Bigg] . \quad (21)$$

The terms for $Rg\bar{Q}^t$ are obtained by replacing $h_n(kr)$ by $j_n(kr)$ in (18)–(21).

IV. Calculations

A computer program was written in Fortran 77 and implemented on a VAX 11/730 and a Cray X-MP/48 to obtain the T matrix for dielectric ellipsoids. The method used to calculate the integrals of (18)–(21) was Gauss quadrature [11]. The order of quadrature and the value of N_{max} must be chosen for each particular case weighing computation time against error.

A number of computational advantages are realized by using the ellipsoidal scatterer instead of the general three-dimensional scatterer. These advantages are implicitly expressed in (18)–(21). In these equations one aspect of the symmetry is accounted for by the bracketed terms multiplying the integrals. These terms, which take on the values of either zero or two, indicate when the integrals need not be carried out. The term $[1 + (-1)^{m'-m}]$ multiplies each of the integrals in (18)–(21) so that none of these integrals needs to be performed when $m' - m$ is odd. The bracketed terms involving $n' + n$ dictate that the integrals in only the $J^{(12)}$ and $J^{(21)}$ expressions should be carried out when $n' + n$ is even, and the integrals in only the $J^{(11)}$ and $J^{(22)}$ expressions should be carried out when $n' + n$ is odd. Equations (18)–(21) also show that when the expressions are nonzero, the integral need only be carried out over one-fourth of the total surface area. These symmetry properties were fully utilized in the computer program to effect a large savings in computation time.

The largest problem undertaken by this program was one involving an N_{max} of 10 and a quadrature order in θ and ϕ of 20. This required approximately 38 s of CPU time when run on a single processor of the four available on a Cray X-MP/48. The majority of this CPU time was spent in the calculations of the elements of $\bar{Q}^t$ and $Rg\bar{Q}^t$. Unfortunately, very little of the code involved in calculating these elements vectorized. Therefore, the supercomputing power of the Cray was not fully realized and this machine essentially served as a powerful mainframe for this program.

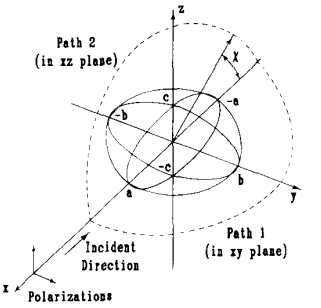

Fig. 1. Diagrammatical representation of scattering problem.

It may be of more interest that when using an N_{max} of 6, giving a T matrix of 96 × 96, and using a quadrature order in θ and ϕ of 20, the T matrix was obtained after 51 min of CPU time on a VAX 11/730. For purposes of comparison, the MicroVAX II, which has approximately three times the computing power of the 11/730, would require roughly 17 min of CPU time to solve this problem.

V. Results

Calculated results are given in this section in terms of the differential cross section of a dielectric ellipsoid under two different polarization conditions. Comparison is made in each case with a dielectric spheroid whose dimensions are comparable to that of the ellipsoid. The size parameter of the ellipsoid is taken to be kl, where k is the wavenumber and l is twice the largest dimension a, b, c of the ellipsoid (Fig. 1).

The calculation time required to obtain the T matrix for an axially symmetric object is much less than that for an ellipsoid since one is characterized by a block-diagonal and the other by a full T matrix. It would seem that an ellipsoid that is nearly axially symmetric might be well approximated as a spheroid. However, this approach could lead to unacceptable results, as will be indicated.

A spheroid whose relative permittivity is $2.14 - j0.036$ is assumed to have dimensions in the ratio $a/c = b/c = 4.912$, with $kl = 3.432$. An ellipsoid having the same relative permittivity but with the a dimension ten percent greater and b dimension ten percent less than that of the spheroid is used for comparison; the volume of the ellipsoid is 99 percent of the volume of the spheroid. A plane wave is incident on the scatterer, propagating in the negative x direction and polarized along the z axis as illustrated in Fig. 1. Evaluation of the differential cross section is done along two paths, the first lying in the xy plane, proceeding from the negative to the positive x axis, and the second lying in the xz plane with the same endpoints. The independent variable χ is the angle of arc, in degrees, along the evaluation paths. The differential cross sections of the two objects are shown in Fig. 2. They are seen to be quite similar when χ is less than approximately 90°. However, the difference is marked for larger angles. Therefore, when backscattering is of interest, approximating this ellipsoid as a spheroid may lead to results which are in error by as much as a factor of two.

Fig. 3 shows the differential cross section for the same situation,

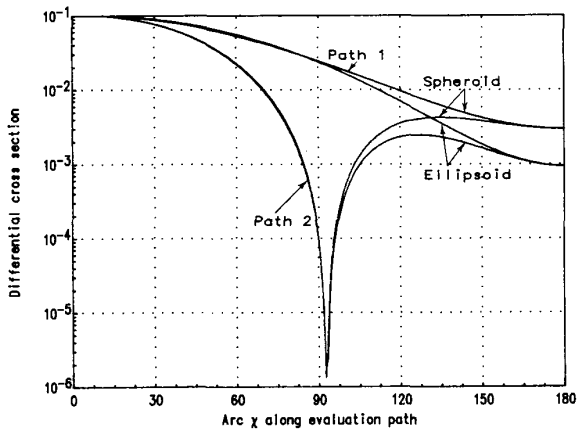

Fig. 2. Differential cross section when incident wave is polarized along z axis.

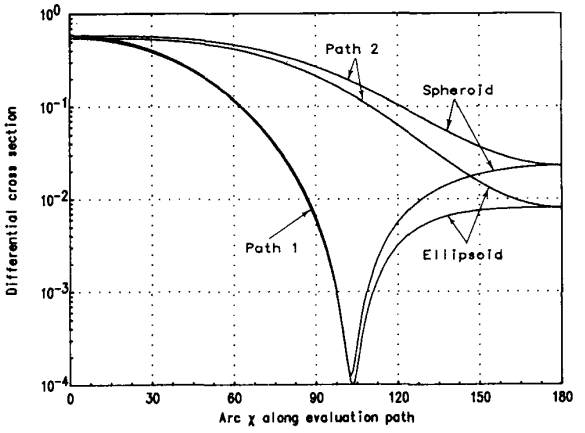

Fig. 3. Differential cross section when incident wave is polarized along y axis.

except the incident plane wave is now polarized along the y axis. As before, the two scatterers appear quite similar in differential cross section when the angle is less than a certain amount, approximately 105° in this case, but strong differences appear beyond this value.

VI. Summary

The extended boundary condition method has been summarized and the dielectric ellipsoid scattering problem formulated in the resonant range. It is thus possible to consider scattering properties of a broader class of targets than those previously found in the literature, specifically those that lack rotational symmetry. Calculated results have been included, and the importance of this extension beyond the rotationally symmetric scatterer is emphasized in terms of a comparison between a dielectric ellipsoid and a spheroid having approximately the same total volume. The importance of differences in the surface and internal propagation paths provided by the two scatterers is evident. More specific interpretations of the differences are difficult to achieve in the resonance region. For example large particle approximations can explain some of the results; small particle approximations interpret others. The inconsistencies appear to be inherent to this region and will be a topic for further study.

The work reported here can provide a basis for further extension to multiple body scattering and also shows promise for categorizing some irregular dielectric shapes in terms of their inclusion in best-fit ellipsoids. This latter aspect is being pursued, as is the immersion of the scatterer in lossy media where it may be especially appropriate for target classification and identification.

Acknowledgment

All values shown in Figs. 2 and 3 were calculated on the Cray X-MP/48 at the San Diego Supercomputer Center.

References

[1] P. C. Waterman, "Symmetry, unitarity, and geometry in electromagnetic scattering," *Phys. Rev. D,* vol. 3, no. 4, pp. 825-839, 1971.
[2] P. Barber and C. Yeh, "Scattering of electromagnetic waves by arbitrary shaped dielectric bodies," *Appl. Opt.,* vol. 14, no. 12, pp. 2864-2872, 1975.
[3] C. Yeh, S. Colak, and P. Barber, "Scattering of sharply focused beams by arbitrarily shaped dielectric particles: an exact solution," *Appl. Opt.,* vol. 21, no. 24, pp. 4426-4433, 1982.
[4] P. W. Barber, J. F. Owen, and R. K. Chang, "Resonant scattering for characterization of axisymmetric dielectric objects," *IEEE Trans. Antennas Propagat.,* vol. 30, no. 2, pp. 168-172, 1982.
[5] A. R. Holt, "The scattering of single hydrometeors," *Radio Sci.,* vol. 17, no. 5, pp. 929-945, 1982.
[6] ——, "Electromagnetic wave scattering by spheroids: A comparison of experimental and theoretical results," *IEEE Trans. Antennas Propagat.,* vol. 30, no. 4, pp. 758-760, 1982.
[7] A. Mugnai and W. Wiscombe, "Scattering from nonspherical Tschebycheff particles. 1: Cross sections, single scattering albedo, asymmetry factor and backscattered fraction," *Appl. Opt.,* vol. 25, no. 7, pp. 1235-1244, 1986.
[8] G. Kristensson and S. Ström, "Electromagnetic scattering from geophysical targets by means of the T matrix approach: A review of some recent results," *Radio Sci.,* vol. 17, no. 5, pp. 903-912, 1982.
[9] A. Karlsson and G. Kristensson, "Electromagnetic scattering from subterranean obstacles in a stratified ground," *Radio Sci.*, vol. 18, no. 3, pp. 345-356, 1983.
[10] L. Tsang, J. A. Kong, and R. T. Shin, *Theory of Microwave Remote Sensing.* New York: Wiley, 1985, pp. 168-186.
[11] M. Abramowitz and I. E. Stegun, *Handbook of Mathematical Functions.* Nat. Bur. Standards, 1972, p. 887.

Scattering from the Perfectly Conducting Cube

MARC G. COTE, MEMBER, IEEE, MARGARET B. WOODWORTH, MEMBER, IEEE AND ARTHUR D. YAGHJIAN, SENIOR MEMBER, IEEE

Abstract—**The scattering cross sections in the E-plane, H-plane, and 45°-plane of the perfectly conducting cube illuminated broadside by an incident plane wave are computed using both a uniform high-frequency diffraction solution and magnetic-field integral equations. The computed cross sections are compared with measured cross sections for cube perimeters of 3, 6, 12, and 20 wavelengths. The total scattering cross section versus the perimeter of the cube is also computed and compared to that of the sphere.**

Manuscript received August 20, 1987; revised February 1, 1988.

M. G. Cote and A. D. Yaghjian are with the Rome Air Development Center, Hanscom Air Force Base, Bedford, MA 01731.
M. B. Woodworth is with the Arcon Corporation, 260 Bear Hill Road, Waltham, MA 02154.

IEEE Log Number 8821493.